

## Isotropic NMR Shifts in Some Pyridine-Type Ligands Complexed with Paramagnetic Undecatungstocobalto(II)silicate and Undecatungstonickelo(II)silicate Anions. Identification of Dumbbell-Shaped 4,4'-Bipyridyl Complexes

Moonhee Ko, Gyung Ihm Rhyu, and Hyunsoo So\*

*Department of Chemistry, Sogang University, Seoul 121-742. Received March 25, 1993*

$^1\text{H}$  and  $^{13}\text{C}$  NMR spectra for pyridine,  $\beta$ - and  $\gamma$ -picoline, pyrazine, and 4,4'-bipyridyl complexed with paramagnetic undecatungstocobalto(II)silicate and undecatungstonickelo(II)silicate anions are reported. For these complexes the ligand exchange is slow on the NMR time scale and the pure resonance lines have been observed at room temperature. The isotropic shifts in nickel complexes can be interpreted in terms of contact shifts by  $\sigma$ -electron delocalization. Both contact and pseudocontact shifts contribute to the isotropic shifts in cobalt complexes. The contact shifts, which are obtained by subtracting the pseudocontact shifts from the isotropic shifts, require both  $\sigma$ - and  $\pi$ -electron delocalization from the cobalt ion. Slow ligand exchange has also allowed us to identify the species formed when bidentate ligands react with the heteropolyanions. Pyrazine forms a 1:1 complex, while 4,4'-bipyridyl forms both 1:1 and dumbbell-shaped 1:2 complexes.

### Introduction

The  $^1\text{H}$  and  $^{13}\text{C}$  NMR spectra of some pyridine-type ligands complexed with paramagnetic bis(2,4-pentanedionato)cobalt(II) and -nickel(II) (hereafter denoted as  $\text{Co}(\text{acac})_2$  and  $\text{Ni}(\text{acac})_2$ , respectively) were reported.<sup>1-3</sup> However, the actual shift for a particular proton or carbon was dependent upon solution composition, indicating that the exchange of ligands between complexed and uncomplexed sites was rapid compared to the separation in resonance frequency for the proton or carbon in diamagnetic and paramagnetic environments. The relative isotropic NMR shifts were interpreted qualitatively in terms of contact and pseudocontact interactions.<sup>1-3</sup> Later Horrocks and Hall determined the absolute isotropic shifts for pyridine coordinated to  $\text{Ni}(\text{acac})_2$  and  $\text{Co}(\text{acac})_2$  by measuring isotropic shifts as a function of the concentration of the coordinated pyridine.<sup>4</sup> They also noted that there was large discrepancy between the relative  $^{13}\text{C}$  isotropic shifts reported by two different groups.

We have found that pyridine-type ligands coordinated to the heteropolyanion  $[\text{SiW}_{11}\text{MO}_{39}]^{6-}$  ( $\text{M} = \text{Co}^{\text{II}}$  or  $\text{Ni}^{\text{II}}$ ; denoted as  $\text{SiW}_{11}\text{M}$  hereafter) undergo slow exchange on the NMR time scale, exhibiting NMR peaks separated from those of free ligands. The slow exchange of some ligands coordinated to  $\text{SiW}_{11}\text{M}$  has allowed us to measure the absolute isotropic NMR shifts directly, and to identify the species formed when bidentate ligands such as pyrazine and 4,4'-bipyridyl react with  $\text{SiW}_{11}\text{M}$ . In this paper we report absolute isotropic NMR shifts of some pyridine derivatives coordinated to  $\text{SiW}_{11}\text{Co}$  and  $\text{SiW}_{11}\text{Ni}$ , and estimate contact and pseudocontact contributions to the isotropic shifts.

### Experimental

$\text{K}_6[\text{SiW}_{11}\text{Co}(\text{H}_2\text{O})\text{O}_{39}] \cdot n\text{H}_2\text{O}$  and  $\text{K}_6[\text{SiW}_{11}\text{Ni}(\text{H}_2\text{O})\text{O}_{39}] \cdot n\text{H}_2\text{O}$  were prepared according to the methods of Simmons<sup>5</sup> and Weakley *et al.*<sup>6</sup>

$^1\text{H}$  NMR (300.08 MHz) and  $^{13}\text{C}$  NMR (75.46 MHz) spectra were obtained in the Fourier-transform mode with a Varian

Gemini-300 7.05 T spectrometer equipped with a broad band, narrow-bore probe. NMR measurements were made at ambient temperature (22-25°C). The line-broadening factor used in exponential apodization was 20 Hz. For  $^1\text{H}$  NMR spectroscopy, 90° pulses (10  $\mu\text{s}$ ) were used, and the acquisition time was 0.2 s. No extra delay time between pulses was introduced. DSS was used as an internal reference. For  $^{13}\text{C}$  NMR spectroscopy, 90° pulses (13  $\mu\text{s}$ ) were used, and the pulse repetition time was 0.3 s with the acquisition time of 0.2 s. Proton was decoupled by Waltz-16 decoupling method. Dioxane was used as an external reference.

### Results and Discussion

**$\text{SiW}_{11}\text{Co}$  Complexes.** The  $^1\text{H}$  NMR spectrum of a  $\text{D}_2\text{O}$  solution containing pyridine and  $\text{SiW}_{11}\text{Co}$  is shown in Figure 1. The three peaks at 8.7, 8.1, and 7.6 ppm are attributed to  $\alpha$ -,  $\gamma$ -, and  $\beta$ -proton of free pyridine, respectively. The three peaks at 113.1, 25.9, and -5.0 ppm, which appear only when  $\text{SiW}_{11}\text{Co}$  is added, are assigned to  $\alpha$ -,  $\beta$ -, and  $\gamma$ -proton of the coordinated pyridine by comparing with the previous assignments<sup>1</sup> for pyridine coordinated to  $\text{Co}(\text{acac})_2$ . Thus the isotropic shifts for  $\alpha$ -,  $\beta$ -, and  $\gamma$ -proton are 104.4, 18.3, and -13.1 ppm, respectively. The plus and minus signs denote the downfield and upfield shifts, respectively. It is noted that these values are much larger than the corresponding values<sup>4</sup> of 32.9, 5.0, and -9.4 ppm for pyridine coordinated to  $\text{Co}(\text{acac})_2$ .

The  $^{13}\text{C}$  NMR spectrum of a  $\text{D}_2\text{O}$  solution containing pyridine and  $\text{SiW}_{11}\text{Co}$  is shown in Figure 2. The three peaks at 151.9, 141.2 and 127.6 ppm are attributed to  $\alpha$ -,  $\gamma$ -, and  $\beta$ -carbon of free pyridine, respectively. The three peaks at 556.8, 59.5, and -90.9 ppm, which appear only when  $\text{SiW}_{11}\text{Co}$  is added, are assigned to  $\beta$ -,  $\gamma$ - and  $\alpha$ -carbon of the coordinated pyridine by comparing with the previous assignments<sup>2</sup> for pyridine coordinated to  $\text{Co}(\text{acac})_2$ . Thus the isotropic shifts for  $\alpha$ -,  $\beta$ -, and  $\gamma$ -carbon are -242.8, 429.2, and -81.7 ppm, respectively.

$\alpha$ -Picoline exhibits no additional peak in the presence of

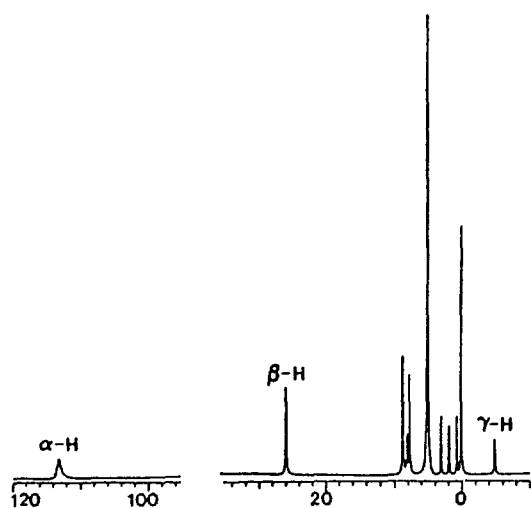


**Figure 1.**  $^1\text{H}$  NMR spectrum of a  $\text{D}_2\text{O}$  solution containing 1:1 pyridine and  $\text{SiW}_{11}\text{Co}$ . Chemical shifts in ppm from TMS. The four peaks at 0-4 ppm come from DSS, and the peak at 4.80 ppm from HDO. The peaks originating from the complex are labeled.

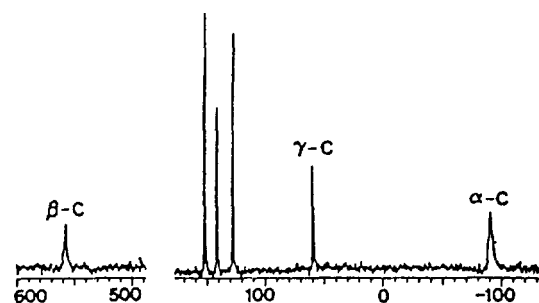


**Figure 2.**  $^{13}\text{C}$  NMR spectrum of a  $\text{D}_2\text{O}$  solution containing 1:1 pyridine and  $\text{SiW}_{11}\text{Co}$ . Chemical shifts in ppm from TMS. The peaks originating from the complex are labeled.

$\text{SiW}_{11}\text{Co}$ , indicating that severe steric hindrance prevents it from coordinating to  $\text{SiW}_{11}\text{Co}$ .  $\beta$ - and  $\gamma$ -picoline behave similarly as pyridine, showing separate peaks for the complexed and free ligands. Peaks have been assigned to particular ligand hydrogen and carbon atoms by comparing with the previous assignments for the  $\text{Co}(\text{acac})_2$  complexes.<sup>1</sup> The NMR peaks and their assignments are listed in Table 1.

The  $^1\text{H}$  NMR spectrum of a  $\text{D}_2\text{O}$  solution containing pyrazine and  $\text{SiW}_{11}\text{Co}$  is shown in Figure 3. The peak at 8.6 ppm belongs to free pyrazine, while two peaks at 88.8 and 17.9 ppm can be assigned to pyrazine coordinated to  $\text{SiW}_{11}\text{Co}$ . If  $\text{SiW}_{11}\text{Co}$  and pyrazine form a 1:1 complex, two peaks with isotropic NMR shifts similar to those of  $\alpha$ - and  $\beta$ -proton in pyridine will appear. If a dumbbell-shaped 2:1 complex is formed, one peak is expected. Therefore, the observed spectrum must come from the 1:1 complex.

The  $^1\text{H}$  NMR spectrum of a  $\text{D}_2\text{O}$  solution containing 4,4'-bipyridyl and  $\text{SiW}_{11}\text{Co}$  is shown in Figure 4. The two peaks at 8.6 and 7.5 ppm are attributed to the 2-H and 3-H of free 4,4'-bipyridyl. The four peaks at 105.8, 19.9, 3.2, and -2.4 ppm are assigned to 2-H, 3-H, 2'-H, and 3'-H of the

**Table 1.** Isotropic NMR Shifts  $\Delta\delta_{\text{iso}}$  of Pyridine-Type Ligands Coordinated to  $[\text{SiW}_{11}\text{Co}^{10}\text{O}_{36}]^{6-}$

Ligand	Nucleus <sup>a</sup>	$\delta_{\text{free}}^b$	$\delta_{\text{comp}}^b$	$\Delta\delta_{\text{iso}}$
Pyridine	$\alpha$ -H	8.7	113.1	104.4
	$\beta$ -H	7.6	25.9	18.3
	$\gamma$ -H	8.1	-5.0	-13.1
	$\alpha$ -C	151.9	-90.9	-242.8
	$\beta$ -C	127.6	556.8	429.2
	$\gamma$ -C	141.2	59.5	-81.7
$\beta$ -Picoline	$\alpha$ -H	8.6	115.8	107.2
	$\alpha'$ -H	8.6	118.0	109.4
	$\beta$ -H	7.7	29.4	21.7
	$\gamma$ -H	8.0	-5.2	-13.2
	$\beta'$ -CH <sub>3</sub>	2.6	-2.3	-4.9
	$\alpha$ -C	146.9	-93.7	-240.6
	$\alpha'$ -C	150.1	-77.1	-227.2
	$\beta$ -C	125.3	560.5	435.2
	$\beta'$ -C	136.0	570.9	434.9
	$\gamma$ -C	139.9	55.7	-84.2
$\gamma$ -Picoline	$\beta'$ -CH <sub>3</sub>	17.4	58.9	41.5
	$\alpha$ -H	8.6	116.3	107.7
	$\beta$ -H	7.6	26.9	19.3
	$\gamma$ -CH <sub>3</sub>	2.6	-11.9	-14.5
	$\alpha$ -C	152.0	-45.7	-197.7
	$\beta$ -C	127.0	568.2	441.2
	$\gamma$ -C	150.0	78.2	-71.8
Pyrazine	$\gamma$ -CH <sub>3</sub>	20.5	35.4	14.9
	2-H	8.6	88.8	80.2
	3-H	8.6	17.9	9.3
4,4'-Bipyridyl	2-H	8.6	105.8	97.2
			(99.8) <sup>y</sup>	(91.2) <sup>y</sup>
	3-H	7.5	19.9	12.4
			(9.4) <sup>y</sup>	(1.9) <sup>y</sup>
	2'-H	8.6	3.2	-5.4
	3'-H	7.5	-2.4	-9.9

<sup>a</sup>For  $\beta$ -picoline, the  $\beta'$ -carbon is that bearing the methyl group.

<sup>b</sup>In ppm relative to the  $^1\text{H}$  or  $^{13}\text{C}$  resonances of TMS. <sup>y</sup>2:1  $\text{SiW}_{11}\text{Co}$ -bipyridyl complex.

4,4'-bipyridyl in the 1:1  $\text{SiW}_{11}\text{Co}$ -bipyridyl complex by comparing with the previous assignment<sup>1</sup> for 4-phenylpyridine coordinated to  $\text{Co}(\text{acac})_2$ . Then the isotropic shifts are 97.2, 12.4, -5.4, and -9.9 ppm for 2-H, 3-H, 2'-H, and 3'-H, respectively.

There are two additional peaks at 99.8 and 9.4 ppm. The relative intensity of these peaks increases with an increase of the ratio  $[\text{SiW}_{11}\text{Co}]/[\text{bipyridyl}]$ , indicating that they originate from the 2:1  $\text{SiW}_{11}\text{Co}$ -bipyridyl complex. If the isotropic shifts by two  $\text{Co}^{2+}$  ions are assumed to be additive, the estimated isotropic shifts are 91.8 (=97.2-5.4), and 2.5 (=12.4-9.9) ppm for 2-H and 3-H. These values agree satisfactorily with the observed values of 91.2 and 1.9 ppm. So the NMR spectrum shows clear evidence for the formation of a dumbbell-shaped 2:1  $\text{SiW}_{11}\text{Co}$ -bipyridyl complex.

**$\text{SiW}_{11}\text{Ni}$  Complexes.** The NMR spectra of the  $\text{SiW}_{11}\text{Ni}$  complexes also exhibited separate lines for the complexed

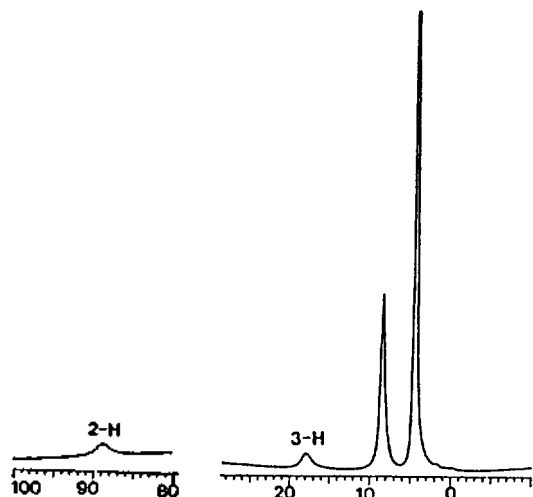


**Figure 3.**  $^1\text{H}$  NMR spectrum of a  $\text{D}_2\text{O}$  solution containing 1:1 pyrazine and  $\text{SiW}_{11}\text{Co}$ . Chemical shifts in ppm from TMS. The peaks originating from the complex are labeled.

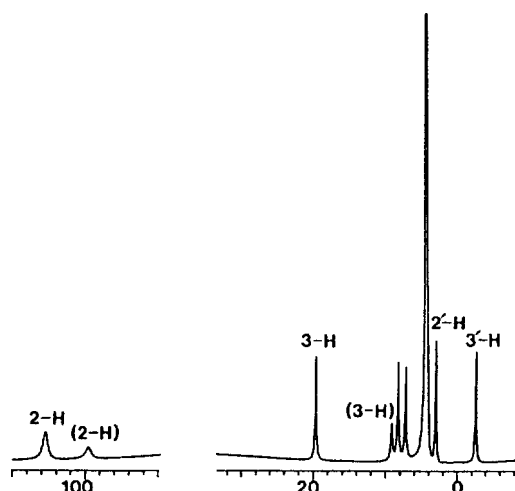


**Figure 4.**  $^1\text{H}$  NMR spectrum of a  $\text{D}_2\text{O}$  solution containing 1:2 4,4'-bipyridyl and  $\text{SiW}_{11}\text{Co}$ . Chemical shifts in ppm from TMS. The peaks originating from the complex are labeled. The two peaks labeled as (2-H) and (3-H) come from the 2:1  $\text{SiW}_{11}\text{Co}$ -bipyridyl complex.

and free ligands. However, their NMR lines were broader than those for the  $\text{SiW}_{11}\text{Co}$  complexes, and the lines originating from the  $\alpha$ -protons were too broad to be observed. The  $^1\text{H}$  NMR spectrum of a  $\text{D}_2\text{O}$  solution containing  $\beta$ -picoline and  $\text{SiW}_{11}\text{Ni}$  and the  $^{13}\text{C}$  NMR spectrum of a  $\text{D}_2\text{O}$  solution containing  $\gamma$ -picoline and  $\text{SiW}_{11}\text{Ni}$  are shown in Figures 5 and 6. The NMR data for the  $\text{SiW}_{11}\text{Ni}$  complexes are listed in Table 2.

**Contact and Pseudocontact Contributions.** The isotropic NMR shifts  $\Delta\delta_{iso}$  in paramagnetic systems contain contact and pseudocontact contributions. Contact shifts occur when unpaired electron density is transferred from the metal to the ligand nucleus in question, whereas pseudocontact shifts arise from a through-space dipolar interaction between

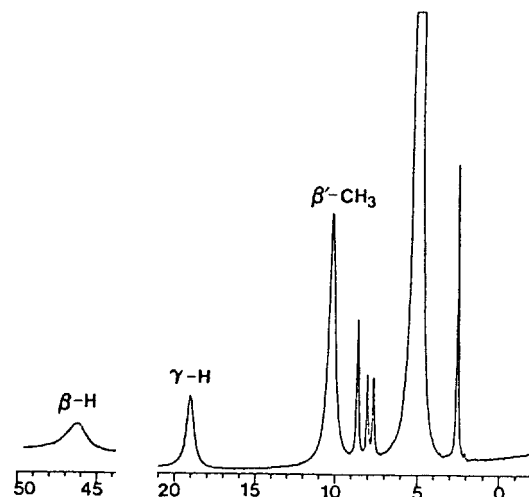


**Figure 5.**  $^1\text{H}$  NMR spectrum of a  $\text{D}_2\text{O}$  solution containing 1:1  $\beta$ -picoline and  $\text{SiW}_{11}\text{Ni}$ . The peaks ascribable to the  $\alpha$ -protons are too broad to be observed. Chemical shifts in ppm from TMS. The peaks originating from the complex are labeled.

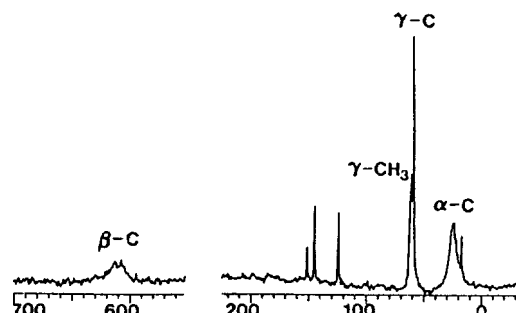


**Figure 6.**  $^{13}\text{C}$  NMR spectrum of a  $\text{D}_2\text{O}$  solution containing 1:1  $\gamma$ -picoline and  $\text{SiW}_{11}\text{Ni}$ . Chemical shifts in ppm from TMS. The peaks originating from the complex are labeled.

the electronic and nuclear magnetic moments.

The pseudocontact shift for a given nucleus  $i$  in an axial system can be expressed as<sup>1</sup>

$$\frac{\Delta\nu_i}{\nu} = -\frac{N_A}{12\pi} \frac{(3\cos^2\theta_i - 1)}{r_i^3} (\chi_{\parallel} - \chi_{\perp}) \quad (1)$$

Here  $N_A$  is Avogadro's constant,  $\theta_i$  is the angle between the principal axis of the complex and the radius vector from the metal ion to the nucleus,  $i$ ;  $r_i$  is the distance between the metal ion and the nucleus,  $i$ ; and  $\chi_{\parallel}$  and  $\chi_{\perp}$  are magnetic susceptibility components parallel and perpendicular to the principal axis.

First we consider the nickel complexes. It has been shown that the pseudocontact contribution to isotropic shifts is small for  $\text{Ni}(\text{acac})_2(\text{ptl})_2$  ( $\text{ptl}$  = pyridine-type ligand).<sup>1-3</sup> For an octahedral  $\text{Ni}(\text{II})$  complex, which has an orbitally non-degenerate  $^3A_{2g}$  ground state with excited states far removed in energy, the orbital contribution is small and so is the magnetic anisotropy. Although  $\text{SiW}_{11}\text{Ni}(\text{ptl})$  deviates considerably from octahedral symmetry, the pseudocontact shifts are expected to be small.

The contact shift  $\Delta\delta_{con}$  can be expressed as

**Table 2.** Isotropic NMR Shifts  $\Delta\delta_{iso}$  of Pyridine-Type Ligands Coordinated to  $[\text{SiW}_{11}\text{Ni}^{\text{II}}\text{O}_{39}]^{6-}$ 

Ligand	Nucleus <sup>a</sup>	$\delta_{\text{free}}^b$	$\delta_{\text{comp}}^b$	$\Delta\delta_{iso}$
Pyridine	$\alpha$ -H	8.7	-	-
	$\beta$ -H	7.6	43.6	36.0
	$\gamma$ -H	8.0	19.8	11.8
	$\alpha$ -C	150.0	6.3	-143.7
	$\beta$ -C	126.1	597	471
	$\gamma$ -C	139.8	57.9	-81.9
$\beta$ -Picoline	$\alpha$ -H	8.6	-	-
	$\alpha'$ -H	8.6	-	-
	$\beta$ -H	7.6	46.1	38.5
	$\gamma$ -H	8.0	19.0	11.0
	$\beta'$ -CH <sub>3</sub>	2.5	10.2	7.7
	$\alpha$ -C	148.9	-7.4	-156.3
	$\alpha'$ -C	152.0	10.0	-142.0
	$\beta$ -C	127.7	606	478
	$\beta'$ -C	138.6	606	467
	$\gamma$ -C	142.7	65.8	-76.9
$\gamma$ -Picoline	$\beta'$ -CH <sub>3</sub>	19.6	53.0	33.4
	$\alpha$ -H	8.6	-	-
	$\beta$ -H	7.6	42.0	34.4
	$\gamma$ -CH <sub>3</sub>	2.6	-9.5	-12.1
	$\alpha$ -C	156.8	29.9	-126.9
	$\beta$ -C	129.8	614	484
	$\gamma$ -C	150.4	65.3	-85.1
Pyrazine	2-H	8.6	-	-
	3-H	8.6	50.1	41.5
4,4'-Bipyridyl	2-H	8.6	-	-
	3-H	7.8	39.8	32.0
			(41.2) <sup>c</sup>	(33.4) <sup>c</sup>
	2'-H	8.6	8.1	-0.5
	3'-H	7.8	9.5	1.7

<sup>a</sup>For  $\beta$ -picoline, the  $\beta'$ -carbon is that bearing the methyl group.  
<sup>b</sup>In ppm relative to the <sup>1</sup>H or <sup>13</sup>C resonances of TMS. <sup>c</sup>2:1 SiW<sub>11</sub>Ni-bipyridyl complex.

$$\Delta\delta_{\text{con}} = \Delta\delta_{\text{con}}^{\pi} + \Delta\delta_{\text{con}}^{\sigma} \quad (2)$$

where  $\Delta\delta_{\text{con}}^{\pi}$  and  $\Delta\delta_{\text{con}}^{\sigma}$  are the contact shifts resulting from the transmission of  $\pi$ - and  $\sigma$ -type electrons. The Ni<sup>2+</sup> ion in octahedral symmetry has two unpaired electrons in  $e_g$  orbitals which have  $\sigma$  symmetry. It is most likely that the unpaired electron density is transferred from the  $d_{z^2}$  orbital to the  $\sigma$  orbital system of the ligand. So isotropic shifts in nickel complexes may be attributed mainly to  $\Delta\delta_{\text{con}}^{\sigma}$ . Horrocks and Johnston have shown that  $\sigma$ -electron delocalization in pyridine derivatives coordinated to Ni(acac)<sub>2</sub> can be interpreted qualitatively by INDO/2 calculations for phenyl, and *o*-, *m*-, and *p*-tolyl radicals.<sup>7</sup> The hyperfine coupling constants,  $A_i$ , calculated by them<sup>7</sup> are compared with the isotropic shifts in SiW<sub>11</sub>Ni(plt) in Table 3. The sign of the shift is predicted correctly for all 20 nuclei. The ratios of the contact shifts to the hyperfine coupling constants ( $\Delta\delta/A_i$ ) within the sets of protons,  $R_H$ , and the sets of carbon nuclei,  $R_C$ , show moderate semiquantitative agreement. (Ideally a single value

**Table 3.** INDO/2 Hyperfine Coupling Constants,  $A_i$ , and Isotropic Shifts<sup>a</sup> for Pyridine-Type Ligands Coordinated to  $[\text{SiW}_{11}\text{Ni}^{\text{II}}\text{O}_{39}]^{6-}$ 

Ligand	Nucleus <sup>a</sup>	$A_i^b$	$\Delta\delta_{iso}^a$	$\Delta\delta/A_i$
Pyridine	$\alpha$ -H	18.7	-	-
	$\beta$ -H	6.1	36.0	5.9
	$\gamma$ -H	3.9	11.8	3.0
	$\alpha$ -C	-4.7	-143.7	30.6
	$\beta$ -C	10.8	471	43.6
	$\gamma$ -C	-2.6	-81.9	31.5
$\beta$ -Picoline	$\alpha$ -H	17.4	-	-
	$\alpha'$ -H	19.3	-	-
	$\beta$ -H	5.7	38.5	6.8
	$\gamma$ -H	4.3	11.0	2.6
	$\beta'$ -CH <sub>3</sub>	1.6	7.7	4.8
	$\alpha$ -C	-4.9	-156.3	31.9
	$\alpha'$ -C	-5.0	-142.0	28.4
	$\beta$ -C	10.7	478	44.7
	$\beta'$ -C	10.4	467	44.9
	$\gamma$ -C	-2.8	-76.9	27.5
$\gamma$ -Picoline	$\beta'$ -CH <sub>3</sub>	0.82	33.4	40.7
	$\alpha$ -H	19.2	-	-
	$\beta$ -H	6.5	34.4	5.3
	$\gamma$ -CH <sub>3</sub>	-1.2	-12.1	10.1
	$\alpha$ -C	-5.1	-126.9	24.9
	$\beta$ -C	10.4	484	46.5
	$\gamma$ -C	-2.3	-85.1	37.0
$\gamma$ -CH <sub>3</sub>	1.4	44.5	31.8	

<sup>a</sup>In ppm. <sup>b</sup>Calculated hyperfine coupling constants in gauss from ref 7.

would be obtained for each set.)

It is noted that  $\Delta\delta/A_i$  values for  $\gamma$ -protons in pyridine and  $\beta$ -picoline are much smaller than the value for  $\beta$ -proton. It is probable that the INDO/2 calculations overestimate the hyperfine coupling constants for  $\gamma$ -protons. The experimental values determined by the EPR spectrum of phenyl radical are 17.4, 6.3, and 2.0 G for  $\alpha$ -,  $\beta$ -, and  $\gamma$ -proton, respectively.<sup>8</sup> It is noted that the experimental value for  $\gamma$ -proton is much smaller than the calculated one. If 3.9 G is replaced by 2.0 G,  $\Delta\delta/A_i$  values for  $\gamma$ -protons (5.9 and 5.5) are now similar to those for  $\beta$ -protons.

It was shown that  $\Delta\delta/A_i$  is inversely proportional to the magnetogyric ratio  $\gamma_N$  of the nucleus involved.<sup>1,12</sup>

$$\Delta\delta/A_i = \frac{\gamma_e}{\gamma_N} \frac{g^2 \mu_B S(S+1)}{3kT} \quad (3)$$

Thus, it follows that

$$\frac{R_C}{R_H} = \frac{\gamma_H}{\gamma_C} = 4.0 \quad (4)$$

The average values of  $R_C$  and  $R_H$  for all carbon atoms and protons in three complexes listed in Table 3 are 35.7 and 6.3,<sup>9</sup> and thus the  $R_C/R_H$  ratio is 5.7. This moderate semiquantitative agreement shows that the observed isotropic shifts for the nickel complexes are due primarily to a contact interaction by  $\sigma$ -electron delocalization.

If the isotropic shifts are determined by  $\sigma$ -electron de-

localization alone, the ratios of the isotropic shifts for corresponding nuclei in two different nickel complexes should be the same. These ratios for  $\text{SiW}_{11}\text{Ni}(\text{py})$  ( $\text{py} = \text{pyridine}$ ), and  $\text{Ni}(\text{acac})_2(\text{py})_2$  are 1.35, 1.48, 1.54, 1.37, and 2.37 for  $\beta\text{-H}$ ,  $\gamma\text{-H}$ ,  $\alpha\text{-C}$ ,  $\beta\text{-C}$ , and  $\gamma\text{-C}$ , respectively. The first four values are quite close, and their average value is 1.44. The isotropic shift for  $\gamma\text{-C}$  in  $\text{Ni}(\text{acac})_2(\text{py})_2$  was calculated from a measured shift of 1.3 ppm with an error of  $\pm 0.3$  ppm.<sup>24</sup> The uncertainty in the experimental value partly accounts for the deviation of the ratio for  $\gamma\text{-C}$ .

The average ratio of 1.4 indicates that  $\sigma$ -electron delocalization is 40% more extensive in  $\text{SiW}_{11}\text{Ni}(\text{py})$  than in  $\text{Ni}(\text{acac})_2(\text{py})_2$ . The unpaired electron from  $d_{z^2}$  orbital in octahedral  $\text{Ni}(\text{acac})_2(\text{py})_2$  is evenly delocalized into two pyridine molecules. The geometry around the nickel ion in  $\text{SiW}_{11}\text{Ni}(\text{py})$  deviates considerably from octahedron. The six oxygen atoms surrounding a tungsten atom in  $[\text{SiW}_{12}\text{O}_{40}]^{4-}$  can be classified into four types: one  $\text{O}_a$  atom shared between three  $\text{WO}_6$  octahedra and the central  $\text{SiO}_4$  tetrahedron, two  $\text{O}_b$  atoms shared between adjacent  $\text{W}_3\text{O}_{13}$  units, two  $\text{O}_c$  atoms shared between two  $\text{WO}_6$  octahedra in the same  $\text{W}_3\text{O}_{13}$  unit, and one  $\text{O}_d$  atom linked to one tungsten atom. The bond lengths are  $\text{W-O}_a$  2.35,  $\text{W-O}_b$  1.92,  $\text{W-O}_c$  1.93, and  $\text{W-O}_d$  1.71 Å.<sup>10</sup> It is noted that the axial  $\text{O}_a$  atom is located 0.4 Å farther than  $\text{O}_b$  and  $\text{O}_c$  atoms which form a square plane. In  $\text{SiW}_{11}\text{Ni}(\text{ptl})$  one of the 12  $\text{W-O}_d$  groups has been replaced by  $\text{Ni}(\text{ptl})$ . Since the  $\text{Ni-O}_d$  bond must be very weak, the geometry around the nickel ion may be considered to be square pyramidal. Therefore the nickel-pyridine bond will be stronger and  $\sigma$ -electron delocalization will be more extensive in  $\text{SiW}_{11}\text{Ni}(\text{py})$  than in  $\text{Ni}(\text{acac})_2(\text{py})_2$ .

The isotropic shifts for the cobalt complexes, which also contain pseudocontact contributions, are more difficult to interpret. In order to separate contact and pseudocontact shifts for  $\text{Co}(\text{acac})_2(\text{py})_2$ , Horrocks and Hall calculated the pseudocontact shifts using the single crystal magnetic susceptibility data.<sup>4</sup> The contact shifts were then determined by subtracting the pseudocontact shifts from the experimental isotropic shifts.

The pseudocontact shift is proportional to the geometrical factor  $(3\cos^2\theta_i - 1)/r_i^3$  and the magnetic anisotropy  $(\chi_{zz} - \chi_{xx})$ ; see Eq. (1). In the absence of the magnetic data for  $\text{SiW}_{11}\text{Co}(\text{ptl})$ , pseudocontact shifts cannot be determined directly. If we assume that the geometrical factors are the same for the given pyridine-type ligand coordinated to  $\text{Co}(\text{acac})_2$  and  $\text{SiW}_{11}\text{Co}$ , the pseudocontact shifts of the latter should be proportional to those of the former. We want to estimate the proportionality constant  $f$ . The pseudocontact shifts for  $f=1$  are listed under  $\Delta\delta_{pc}$  in Table 4. The values for  $\beta'\text{-CH}_3$  of  $\beta$ -picoline,  $\gamma\text{-CH}_3$  of  $\gamma$ -picoline, and  $2'\text{-H}$  and  $3'\text{-H}$  of 4,4'-bipyridyl were calculated from the X-ray data of  $\text{Co}(\text{acac})_2(\text{py})_2$ <sup>11</sup> and the following bond lengths: methyl-ring C-C 1.53, methyl C-H 1.09, ring-ring C-C 1.46 Å.

The contact shifts,  $\Delta\delta_{con}^{\text{Co}}(f=1)$ , are obtained by subtracting the pseudocontact shifts for  $f=1$  from the experimental isotropic shifts. It is noted that some contact shifts of  $\text{SiW}_{11}\text{Co}(\text{ptl})$  based on  $f=1$  are quite similar to the corresponding  $\Delta\delta_{con}^{\text{Ni}}$  values. We have tried to determine the best  $f$  value by comparing the contact shifts of  $\text{SiW}_{11}\text{Co}(\text{ptl})$  with  $\Delta\delta_{con}^{\text{Ni}}$ . The  $\text{Co}^{2+}$  ion in octahedral symmetry has two unpaired electrons in  $e_g$  orbitals which have  $\sigma$  symmetry and one unpaired

**Table 4.** Isotropic, Pseudocontact, and Contact Shifts of Pyridine-Type Ligands Coordinated to  $[\text{SiW}_{11}\text{Co}^{II}\text{O}_{39}]^{6-}$

Ligand	Nucleus	$\Delta\delta_{iso}^{\text{Co}}$	$\Delta\delta_{pc}^{\text{Co}}$	$\Delta\delta_{con}^{\text{Co}}$ ( $f=1$ )	$\Delta\delta_{con}^{\text{Co}}$ ( $f=0.94$ )	$\Delta\delta_{con}^{\text{Ni}}$
Pyridine	$\alpha\text{-H}$	104.4	-39.5	143.9	141.5	-
	$\beta\text{-H}$	18.3	-18.1	36.4	35.3	36.0
	$\gamma\text{-H}$	-13.1	-15.6	2.5	1.6	11.8
	$\alpha\text{-C}$	-242.7	-92.5	-150.0	-155.8	-143.7
	$\beta\text{-C}$	429.1	-35.7	464.8	462.7	471
	$\gamma\text{-C}$	-81.8	-28.3	-53.5	-55.2	-81.9
$\beta$ -Picoline	$\alpha\text{-H}$	107.2	-39.5	146.7	144.3	-
	$\alpha'\text{-H}$	109.4	-39.5	148.9	146.5	-
	$\beta\text{-H}$	21.7	-18.1	39.8	38.7	38.5
	$\gamma\text{-H}$	-13.2	-15.6	2.4	1.5	11.0
	$\beta'\text{-CH}_3$	-4.9	-9.9	5.0	4.4	7.7
	$\alpha\text{-C}$	-240.6	-92.5	-148.1	-153.7	-156.3
	$\alpha'\text{-C}$	-227.2	-92.5	-134.7	-140.3	-142.0
	$\beta\text{-C}$	435.2	-35.7	470.9	468.8	478
	$\beta'\text{-C}$	434.9	-35.7	470.6	468.5	467
$\gamma$ -Picoline	$\gamma\text{-C}$	-84.2	-28.3	-55.9	-57.6	-76.9
	$\beta'\text{-CH}_3$	41.5	-13.6	55.1	54.3	33.4
	$\alpha\text{-H}$	107.7	-39.5	147.2	144.8	-
	$\beta\text{-H}$	19.3	-18.1	37.4	36.3	34.4
	$\gamma\text{-CH}_3$	-14.5	-10.0	-4.5	-5.1	-12.1
	$\alpha\text{-C}$	-197.7	-92.5	-105.2	-110.8	-126.9
	$\beta\text{-C}$	441.2	-18.1	459.3	458.2	484
	$\gamma\text{-C}$	-71.8	-28.3	-43.5	-45.2	-85.1
	$\gamma\text{-CH}_3$	14.9	-12.6	27.5	26.7	44.5
4,4'-Bipyridyl	2-H	97.2	-39.5	136.7	134.3	-
	3-H	12.4	-18.1	30.5	29.4	32.0
	2'-H	-5.4	-4.0	-1.4	-1.6	-0.5
	3'-H	-9.9	-9.0	-0.9	-1.4	1.7

<sup>a</sup>The pseudocontact shifts of pyridine-type ligands coordinated to  $\text{Co}(\text{acac})_2$  from ref 4. Some values have been estimated from the geometry of each complex; see the text.

electron in  $t_{2g}$  orbitals which have  $\pi$  symmetry. Let us first assume that the contact shifts of  $\text{SiW}_{11}\text{Co}(\text{ptl})$  arise due to the  $\sigma$ -electron delocalization alone. Then  $\Delta\delta_{con}^{\text{Co}}$  should be proportional to  $\Delta\delta_{con}^{\text{Ni}}$ . This relation may be expressed as

$$\Delta\delta_{iso}^{\text{Co}} - f \times \Delta\delta_{pc}^{\text{Co}} = g \times \Delta\delta_{con}^{\text{Ni}} \quad (5)$$

where  $f$  and  $g$  are proportionality constants. We have calculated the absolute values of  $(\Delta\delta_{iso}^{\text{Co}} - f \times \Delta\delta_{pc}^{\text{Co}} - g \times \Delta\delta_{con}^{\text{Ni}})$  for various  $f$  and  $g$  values. The minimum average value of 9.4 was obtained for  $f=0.94$  and  $g=0.98$ . A smaller minimum average value of 6.1 was obtained for  $f=0.94$  and  $g=0.98$  when  $\gamma\text{-H}$ ,  $\gamma\text{-C}$ , and  $\gamma\text{-CH}_3$  were not included; see below.

The contact shifts for  $f=0.94$  are listed in Table 4. It is noted that the fit between  $\Delta\delta_{con}^{\text{Co}}$  and  $\Delta\delta_{con}^{\text{Ni}}$  improves slightly when  $f$  is varied. These results show that the  $\sigma$ -electron delocalization alone is not sufficient to explain the contact shift data of  $\text{SiW}_{11}\text{Co}(\text{ptl})$ . Now we include the  $\pi$ -electron delocalization from metal  $t_{2g}$  orbitals. Cramer and Drago used EHMO method to calculate the hyperfine coupling constants for one unpaired electron in  $\pi$  orbitals of pyridine-type li-

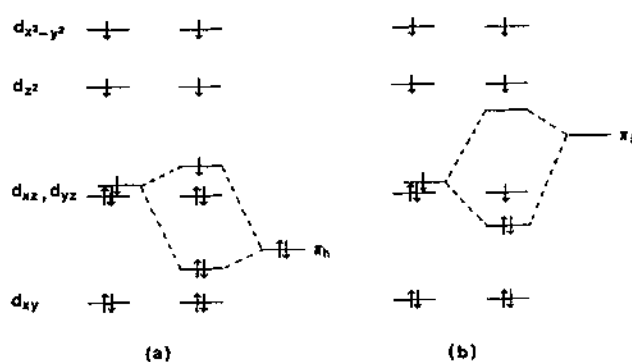


**Figure 7.** Relative energies of 3d orbitals of  $[\text{SiW}_{11}\text{Co}(\text{ptl})\text{O}_{39}]^{6-}$ , when  $d_{xz}$  orbital mixes with (a) a filled  $\pi$  molecular orbital, and (b) a vacant  $\pi$  molecular orbital.

**Table 5.** Hyperfine Coupling Constants in Gauss for One Unpaired Electron in Various Orbitals of Pyridine-Type Ligands

Ligand	Nucleus	$\pi_h^a$	$\pi_f^b$	$\sigma$
Pyridine	$\alpha$ -H	-1.51	2.05	17.4 <sup>c</sup>
	$\beta$ -H	-1.60	0.87	6.3 <sup>b</sup>
	$\gamma$ -H	-6.20	5.58	2.0 <sup>b</sup>
$\gamma$ -Picoline	$\alpha$ -H	-1.75	2.92	19.2 <sup>c</sup>
	$\beta$ -H	-2.33	1.42	6.5 <sup>b</sup>
	$\gamma$ -CH <sub>3</sub>	+6.80	-4.31	-1.2 <sup>c</sup>

<sup>a</sup>EHMO calculation data from ref. 12.  $\pi_h$  and  $\pi_f$  represent HOMO and LUMO  $\pi$  orbitals. The signs are for a  $\beta$  spin in the  $\pi_h$  orbital and an  $\alpha$  spin in the  $\pi_f$  orbital. <sup>b</sup>EPR data from ref. 8. <sup>c</sup>INDO/2 calculation data from ref. 7.

gands coordinated to nickel(II) complexes.<sup>12</sup> Nickel complexes have no unpaired electron in  $t_{2g}$  orbitals. When a ligand  $\pi$  molecular orbital mixes with a filled  $t_{2g}$  orbital, spin polarization on the metal delocalizes  $\alpha$  spin in the  $\pi$  molecular orbital and  $\beta$  spin is placed on the hydrogen atom by spin polarization. They presented calculated hyperfine coupling constants for this case.<sup>13</sup>

The situation is more complicated for  $\text{SiW}_{11}\text{Co}(\text{ptl})$ . The geometry around the cobalt ion in  $\text{SiW}_{11}\text{Co}(\text{ptl})$  is close to square pyramid, as was discussed before for the nickel ion in  $\text{SiW}_{11}\text{Ni}(\text{ptl})$ . Therefore the  $d_{xy}$  orbital has the lowest energy among  $t_{2g}$  orbitals<sup>14</sup> (Figure 7). If there were no  $\pi$  interaction between the metal and pyridine-type ligand,  $d_{xz}$  and  $d_{yz}$  orbitals would be degenerate. If one of them (say, the  $d_{xz}$  orbital) mixes with a filled  $\pi$  orbital, the molecular orbital containing the  $d_{xz}$  orbital will have higher energy than the  $d_{yz}$  orbital, and thus have the unpaired electron. In this case  $\beta$  spin is delocalized into the  $\pi$  molecular orbital and  $\alpha$  spin is placed on the hydrogen atoms. On the other hand, if the  $d_{xz}$  orbital mixes with a vacant  $\pi$  orbital, the molecular orbital containing the  $d_{xz}$  orbital will have lower energy than the  $d_{yz}$  orbital, and thus have paired electrons. In this case  $\alpha$  spin is delocalized into the  $\pi$  molecular orbital by spin polarization and  $\beta$  spin is placed on the hydrogen atoms. In each case the hydrogen atoms in CH<sub>3</sub> group have the same spin as the  $\pi$  molecular orbital by hyperconjugation. Our NMR data are consistent with the former case, as will be shown

later. So we have listed the hyperfine coupling constants calculated by Cramer and Drago<sup>12</sup> with changed signs for the lowest unoccupied  $\pi$  molecular orbitals (LUMO) in Table 5.

It is noted that direct  $\pi$ -electron delocalization in the ligand highest occupied  $\pi$  molecular orbital (HOMO) causes opposite shifts from that of the  $\sigma$ -electron delocalization, and that it has most pronounced effects on  $\gamma$ -H and  $\gamma$ -CH<sub>3</sub>. Let us compare calculated  $\Delta\delta_{\text{iso}}^{\text{Co}}$  values with  $\Delta\delta_{\text{iso}}^{\text{Ni}}$  for  $\gamma$ -H and  $\gamma$ -CH<sub>3</sub> in Table 4. Compared with  $\Delta\delta_{\text{iso}}^{\text{Ni}}$ ,  $\Delta\delta_{\text{iso}}^{\text{Co}}$  is about 10 ppm smaller for  $\gamma$ -H and 7 ppm larger for  $\gamma$ -CH<sub>3</sub>. This is exactly what is expected when a small amount of  $\pi$ -electron delocalization in HOMO is involved, whereas any  $\pi$ -electron delocalization in LUMO would shift the  $\Delta\delta_{\text{iso}}^{\text{Co}}$  values in wrong directions.

To make it more quantitative, we assume that  $\Delta\delta_{\text{iso}}^{\text{Ni}}$  is the same as the contact shift by  $\sigma$ -electron delocalization in the cobalt complexes. Then we get the following relation

$$\Delta\delta_{\text{iso}}^{\text{Co}} - f \times \Delta\delta_p - h \times A_n = \Delta\delta_{\text{iso}}^{\text{Ni}}$$

where  $f$  and  $h$  are proportionality constants, and  $A_n$  is the hyperfine coupling constant for one unpaired electron in HOMO. When the values for  $\gamma$ -H in pyridine and  $\gamma$ -CH<sub>3</sub> in  $\gamma$ -picoline are used, the following simultaneous equations are obtained.

$$\begin{aligned} -13.1 + 15.6f + 6.20h &= 11.8 \\ -14.5 + 10.0f - 6.80h &= -12.1 \end{aligned}$$

Solution of this set of equations yields  $f=1.10$  and  $h=1.26$ . Using the hyperfine coupling constants for  $\gamma$ -H in Table 5, we calculate from  $h=1.26$  that the unpaired electron density in the  $\pi$  molecular orbital is 21% for that in the  $\sigma$  molecular orbital.

In summary, we have shown that  $\sigma$ -electron delocalization is the dominant mechanism for the isotropic shifts of pyridine-type ligands coordinated to  $\text{SiW}_{11}\text{Ni}$ . For the  $\text{SiW}_{11}\text{Co}$  complexes both contact and pseudocontact contributions are important. When appropriate pseudocontact shifts are subtracted from the isotropic shifts, the resulting contact shifts require both  $\sigma$ - and  $\pi$ -electron delocalization. We have also shown that 4,4'-bipyridyl forms both 1:1 and 2:1  $\text{SiW}_{11}\text{M}$ -bipyridyl complexes.

**Acknowledgment.** The financial support of the Korea Science and Engineering Foundation is gratefully acknowledged. The use of NMR spectrometer is financially supported by the Organic Chemistry Research Center.

## References and Notes

- J. A. Happe and R. L. Ward, *J. Chem. Phys.*, **39**, 1211 (1963).
- D. Doddrell and J. D. Roberts, *J. Amer. Chem. Soc.*, **92**, 6839 (1970).
- I. Morishima, T. Yonezawa, and K. Goto, *J. Amer. Chem. Soc.*, **92**, 6651 (1970).
- W. DeW. Horrocks, Jr. and D. Dew. Hall, *Inorg. Chem.*, **10**, 2368 (1971).
- V. E. Simmons, Ph. D. Thesis, Boston University (1963).
- T. J. R. Weakley and S. A. Malik, *J. Inorg. Nucl. Chem.*, **29**, 2935 (1967).

7. W. DeW. Horrocks, Jr. and D. L. Johnston, *Inorg. Chem.*, **10**, 1835 (1971).
8. H. Zemel and R. W. Fessenden, *J. Phys. Chem.*, **79**, 1419 (1975).
9.  $A_i = 2.0$  G was used for  $\gamma$ -protons in pyridine and  $\beta$ -picoline to get these values.
10. F. Robert, A. Tézé, G. Herve, and Y. Jeannin, *Acta. Cryst.*, **B36**, 11 (1980).
11. R. C. Elder, *Inorg. Chem.*, **7**, 1117 (1968).
12. R. E. Cramer and R. S. Drago, *J. Amer. Chem. Soc.*, **92**, 66 (1970).
13. Cramer and Drago also calculated the hyperfine coupling constants by  $\sigma$ -electron. But EHMO calculations on  $\sigma$  electron do not produce good results; see ref 7.
14. B. Bosnich, W. G. Jackson, and S. T. D. Lo, *Inorg. Chem.*, **14**, 2998 (1975).

## Photochemistry of Conjugated Polyacetylenes. Photoreaction of 1,4-Diphenylbutadiyne with a Mixture of Olefins

Chang Beom Chung, Geon-Soo Kim, Jang Hyuk Kwon, and Sang Chul Shim\*

*Department of Chemistry, Korea Advanced Institute of Science and Technology, Taejeon 305-701*

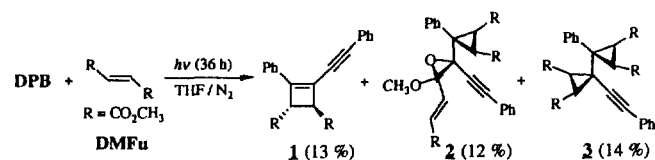
*Received April 12, 1993*

Irradiation of 1,4-diphenylbutadiyne (DPB) with a mixture of electron-deficient and electron-rich olefins in deaerated tetrahydrofuran yields a 1:1 primary photoadduct between DPB and electron-deficient olefins. Irradiation of the primary photoadduct of DPB and dimethyl fumarate (DMFu) with various olefins such as DMFu, acrylonitrile (AN), and 2,3-dimethyl-2-butene (DMB) in deaerated tetrahydrofuran yields regiospecific 1:1 photoadducts. The electron-deficient olefins are more reactive than electron-rich olefins in the photoreaction which proceeds through excited triplet state.

### Introduction

The [2+2] photocycloaddition reaction of olefins has been extensively studied and the reaction mechanisms have been well understood. On the contrary, the photoreaction of acetylenes with olefins received relative little attention. There are a few reports of photocycloaddition reactions of acetylenes with olefins.<sup>1-5</sup> In most cases cyclobutene rings are formed, but cyclopropyl photoadducts as minor products were also observed.<sup>6-8</sup> When two alkene units are incorporated into a rigid molecule, such as cyclohexa-1,4-diene, the major photoproduct was the bicyclopropyl adduct.<sup>7,8</sup> From sensitizing and triplet quenching studies on the formation of cyclobutene photoproduct, the photoreaction is suggested to proceed through the lowest triplet excited state of acetylene. The formation of cyclopropyl photoproduct is proposed to be concerted.

We have previously reported interesting photoreactions of 1:1 1,4-diphenylbutadiyne (DPB) with several olefins to yield 1:1 and 1:2 photoadducts.<sup>9-11</sup> The photoreaction of DPB with dimethyl fumarate (DMFu) in deaerated THF solution at 300 nm yields one primary 1:1 photoadduct (**1**) and two secondary 1:2 photoadducts (**2** and **3**).<sup>11</sup>



Triplet quenching experiments showed that the photoreaction of DPB with DMFu to give **1** proceeds *via* triplet excited state of DPB and **2** and **3** are produced *via* singlet and triplet excited states of **1**, respectively. The photoadduct **2** very interestingly possessed a cyclopropane and an oxirane ring and a triplet carbene intermediate is proposed for **3** in a plausible mechanism.

In this investigation, we report regiospecific photocycloaddition reactions of DPB or **1** with electron-deficient and electron-rich olefins and the relative reactivity of some olefins.

### Results and Discussion

Irradiation of **1** with olefins in deaerated tetrahydrofuran at 300 nm yields 1:1 photoadducts and trace amount of **1'** (<1%), a configurational isomer of **1**. The structure of these adducts was determined by various physical methods such as UV, IR, NMR, and MS spectroscopy.

Some photoadducts are obtained when **1** is irradiated in deaerated tetrahydrofuran solutions of various olefins such as DMFu, AN, and DMB.

The UV spectra of **7** and **8** are quite different from those of **4**, **5**, and **6** which are very similar to each other indicating that these adducts have the same chromophore (Figure 1). The absorption maxima were slightly blue shifted in **4**, **5**, and **6** and considerably in **7** and **8**. IR spectra of **4** and **5** show a C≡N stretching band while **6-8** show no acetylenic stretching band. The significant difference of IR spectra of **6** and **7** (or **8**) is the C=C stretching band at  $\sim 1600 \text{ cm}^{-1}$ . Mass spectra of all the photoproducts show molecular ion peaks indicating that all the products are formed by the ad-

\*To whom correspondence should be addressed